



## Modifications to Walker-Anderson Model for Analysis of High-velocity Penetration of an Eroding Long-rod Projectile into Semi-infinite Concrete Targets

M. Zolfaghari\*

Department of Mechanical Engineering, Arak University, Arak, Iran

### PAPER INFO

#### Paper history:

Received 12 July 2016

Received in revised form 08 August 2016

Accepted 10 March 2017

#### Keywords:

Eroding Projectile  
Concrete Resistance  
Analytical Model  
Long Rod  
Penetration

### ABSTRACT

This paper presents a modified form of the Walker-Anderson (W-A) model for analyzing high velocity penetration of an eroding projectile into a concrete target in which the W-A model is improved by incorporating calculations for the plastic flow field of concrete in terms of its compressibility and strain rate sensitivity under severe pressure. With the changes to and calculations of plastic field in concrete targets, equations of penetration were rearranged. Solution of equations gives penetration depth, penetration velocity, projectile rod velocity and length of a projectile instantaneously. Results of this analysis were compared with experiments performed by authors of this paper. Experiments were performed in order to test eroding long-rod ( $9 \leq L/d \leq 11$ ) penetration into semi-infinite concrete targets at high impact velocities ( $650 \text{ (m/s)} < v < 1150 \text{ (m/s)}$ ). Comparisons show overall agreement between results of the analysis and experiments (average error was 12%). In cases where it is not possible to perform the experiments, the results of the modified model have been compared with the numerical simulations performed by the authors in the literature. Parametric study performed in this paper showed that the two parameters- "plastic flow field characteristic  $\alpha$ " around the projectile tip in the target and unconfined compressive strength of the concrete- are two key parameters influencing the results. The study showed that the level of importance of plastic flow field characteristic is high in forming the resistance against eroding penetration and its effect is not less than the unconfined compressive strength of concrete.

doi: 10.5829/idosi.ije.2017.30.05b.18

## 1. INTRODUCTION

Resisting forces that target applies against projectile penetration, is one of the most important parameters in formulating penetration models. When a long-rod projectile strikes a semi-infinite concrete target, its linear momentum decreases due to target resistance. Since the momentum is defined as the product of mass and velocity, in the case of eroding, projectile the effects of both mass and velocity should be considered in formulating the target's resistance to penetration. There were several approaches for the analysis of eroding penetration into the infinite targets. The improved Tate model uses the flow field pattern in a semi-infinite solenoid [1]; the Vahedi model

concentrates on erosion [2]; the Luk and Piekutowski model is based on a mushroomed nose form of projectile in high-velocity penetrations [3], and the Yarin model is based on the flow pattern formation over an ovoid nose in an eroding penetration using a combination of steady flow and a source [4, 5]. Although each of these models has superiorities compared to others, none of them has the capability of a reference model. Tate's model was known as an important reference in the past five decades due to simplicity of equations and precise phenomenology.

In the case of concrete targets, which is the concern of the present paper, proposed models by other authors were concentrated on rigid penetration of the projectile into the target. Based on these models, the most comprehensive of which is the Forrestal model [6-8], equations developed based on the resistance against expansions of spherical cavity-creation (based on cavity

\*Corresponding Author's Email: m-zolfaghari@araku.ac.ir (M. Zolfaghari)

expansion theory) were used to estimate forces on spherical-shaped punch noses pushed into concrete targets. According to the cavity expansion theory, the motion of target material can be viewed as a continuous expansion of a series of imaginary cavities, which initially have zero radius and then expand to a size that permits passage of the penetrator.

These models have considered only compressibility and cracking properties of concrete but some important phenomena such as compressibility under severe confinements, strain rate and viscose properties of concrete particles at high pressures did not appear in the equations of the models [6, 7]. These deficiencies cause the inability of the models to precisely describe target resistance against the penetration process with respect to material flow around the eroding projectile tip. Furthermore, Forrestal showed that the strength parameter ( $s_f'$ ) cannot express the constant part of penetration resistance due to its dependency on geometry and dimensions of the target. He introduced the resistance of the target parameter R instead of  $s_f'$  in order to overcome this dependency [8]. Since parameter R is obtained from each case of the penetration tests, comprehensiveness of the model is under question. In consideration of strain rate and locking behavior of concrete [9-11], Gao made attempts to interpret penetration resistance behavior of the concrete by presenting a comprehensive model [12]. However, his model could not describe rationally the target resistance to penetration due to ambiguity in the calculation of the shock affected regions, dispersion in results and non-consideration of the projectile erosion. Gao's model can correctly predict severe changes of acceleration of the projectile during rigid penetration.

In this paper, an attempt is made to present an analytical model for penetration of eroding long-rod projectiles into semi-infinite concrete targets. The model utilizes similarities in the quality of flow field around the projectile tip between eroding penetration of long rods into the metallic and concrete targets associated with inserting some improvements into the W-A model. The inserted changes make the W-A model suitable for the analysis of eroding penetration into concrete targets.

Therefore, the viscoplastic material model is used to describe the flow field around the penetrating projectile tip. This material model has the ability to describe concrete behavior under high pressure, confinements and high strain rates. The model considers the effects of erosion and strain rate and can predict the thickness of the incompressible layer ( $\Delta$  in Figure 1). Therefore, considering the effect of erosion and the rate of strain, the constrains in the Forrestal model for applying to high impact velocities will be overcome.

## 2. FORMULATION OF RESISTANCE OF A CONCRETE TARGET AGAINST A HIGH-VELOCITY ERODING LONG-ROD PROJECTILE

Numerical simulations show that the velocity of the projectile rod and pressure at the projectile-target interface are approximately constant during the penetration process. This is true for both metallic and concrete targets [13-15]. Therefore, a momentum equation can be written for eroding penetration of a long-rod projectile into a concrete target. A schematic view for penetration of a long rod into a semi-infinite concrete target is shown in Figure 1. The dashed lines in Figure 1 show the boundaries between incompressible plastic, compressible plastic and elastic regions. These regions are formed due to shock waves during penetration of an eroding long rod into a concrete target [16].

The momentum equation in the axial direction  $z$  in Eulerian coordinates is written as follows:

$$\frac{\partial v_z}{\partial t} + v_r \frac{\partial v_z}{\partial r} + v_z \frac{\partial v_z}{\partial z} = \frac{1}{\rho} \left( \frac{\partial \sigma_{zz}}{\partial z} + \frac{\partial (\sigma_{rz} + p)}{\partial r} + \frac{(\sigma_{rz} + p)}{r} \right) \quad (1)$$

where  $\sigma_{ij} = -p + S_{ij}$  stress tensor    Hydrostatic term    Deviatoric term  $\xrightarrow{so} S_{rz} = \sigma_{rz} + p$  Assuming steady penetration, Walker- Anderson proved that Equation (1) could be written as [17, 18] (see Figure 1):

$$\rho v_z \frac{dv_z}{dz} = \frac{d}{dz} (S_{zz} - p) + 2 \frac{\partial S_{rz}}{\partial r} \Big|_{r=0} \quad r=0, \quad z_0 - \ell \leq z \leq z_{ep} \quad (2)$$

In Equation (2),  $\ell$  is instantaneous projectile length and  $z_0$  and  $z_{ep}$  are target-projectile interface and elastic-plastic position, respectively. Integrating Equation (2) between the target-projectile interface and an arbitrary point in plastic region yields:

$$p(z_0) = \underbrace{\int_{z_0}^z \rho v_z dv_z}_{R_h} + p(z) + S_{zz}(z_0) - S_{zz}(z) - 2 \int_{z_0}^z \frac{\partial S_{rz}}{\partial r} \Big|_{r=0} dz \quad (3)$$

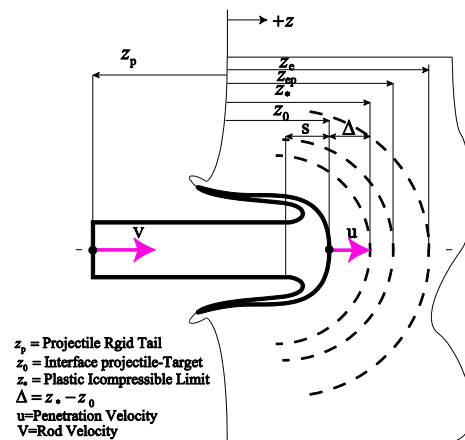


Figure 1. Schematic view of eroding penetration of a long rod into a semi-infinite concrete target

The integral denoted by  $R_h$  is hydrodynamic pressure at the target-projectile interface. Since concrete is a compressible material, density changes must be included in  $R_h$ . Investigations show that due to the impact of the nose of the projectile at the surface of the penetration cavity, a region with diameter as large as the projectile diameter is constructed around the tip of the projectile and the huge pressure of the region closes all of the concrete cavities so that concrete becomes incompressible and exhibits *lock behavior* in the region. The main characteristic of this region is incompressibility, having a pressure greater than or equal to the *locking pressure*  $p_u$  and severe hardening of the concrete material [13, 16, 18]. Therefore, density changes to *lock density* in the first term of Equation (3) and the outcome from the integral could be calculated as the pressure at the target-projectile interface. Coordinates of the point at the incompressible-plastic compressible boundary are specified by  $z_*$  in Figure 1.

$$p(z_0) = \underbrace{\frac{1}{2}\rho_t v_z^2(z_*) - \frac{1}{2}\rho_t v_z^2(z_0)}_{\Delta R_h} + p(z_*) + \underbrace{S_{zz}(z_0) - S_{zz}(z_*)}_{\Delta S_{zz}} - 2 \int_{z_0}^{z_*} \underbrace{\frac{\partial S_{rz}}{\partial r}}_{R_s} \Big|_{r=0} dz \quad (4)$$

Determination of parameters  $v_z$  at  $z=z_0$  &  $z=z_*$ ,  $p(z_*)$  and  $S_{zz}$  at  $z=z_0$  &  $z=z_*$  and  $S_{rz}(z)$  in general involve a numerical solution for equations of mass conservation, momentum and energy conservation. In a simple axisymmetric case, there is an analytical solution for  $S_{zz}$  which shows that  $\Delta S_{zz}=0$ . It can be concluded from Equation (4) that pressure at the target-projectile interface is related to a variation of hydrodynamic pressure  $R_h$ , pressure at the incompressible-compressible boundary and the radial gradient of shear stress. Several simulations have determined that the following parameters make the biggest contribution to pressure at the target-projectile interface: hydrodynamic pressure  $R_h$ , pressure at the incompressible-compressible boundary  $p(z_*)$  and the integral of the radial gradient of shear stress  $R_s$ . A comparison of Equations (3-4) with the Bernoulli equation in Tate's model, clarifies the strength nature of  $R_t$  in that model for concrete targets. Tate's equation for a penetrating projectile is [19]:

$$Y_p + \frac{1}{2}\rho_p(v-u)^2 = \frac{1}{2}\rho_t u^2 + R_t \quad (5)$$

In the above equation,  $Y_p$ ,  $\rho_t$  and  $\rho_p$  are dynamic strengths of the projectile, densities of the target and projectile, respectively. Comparing Equations (3-5) one can write:

$$\frac{1}{2}\rho_t u^2 = \int_{z_0}^{z_*} \rho_t v_z dv_z \quad (6)$$

$$R_t = p(z_*) - 2 \int_{z_0}^{z_*} \frac{\partial S_{rz}}{\partial r} \Big|_{r=0} dz \quad (7)$$

Penetration of an eroding long rod into a concrete target is analyzed using Equations (1-7). The analysis clarifies

the nature of the resisting force  $R_h$  (hydrodynamic pressure, which is related to the velocity of the penetration) and  $R_s$  (constant term of strength, which is not  $f'_c$  and is not proportional to it) against penetration of an eroding long rod into a concrete target.

In order to make a real insight into the process, the quantitative order of resistance parameters and calculation of plastic flow and penetration parameters of the eroding long rod into the semi-infinite concrete target are simulated.

### 3. SIMULATION OF PENETRATION OF AN ERODING LONG ROD INTO A CONCRETE TARGET

In order to make a precise evaluation of eroding penetration of long rods into concrete targets and validation of the proposed model, simulations were performed using the Autodyn software. Firstly, validity of the code is evaluated by simulating a reference test. Based on this, the results of the simulation (penetration depth, residual mass and history of the position of penetrating projectile tip) were compared with reference test results [14]. The validation method is described with the relevant details in reference [16]. Figure 2 shows the comparison between performed numerical simulations and test results from reference [14]. As can be seen, there is an approximately uniform difference between simulations and test results. The average of the error values for depth of penetration and residual mass is equal to 6.5%.

After assurance of the simulation process, simulations were carried out for penetration of copper long rods with a diameter of 19cm and length to diameter ratio of 14.6. The average strength of cylindrical concrete target samples was 37.4 MPa. Striking velocities were considered between 500 and 2500m/s with a 100m/s increment. The material model for concrete was the RHT model which has the advantage of high sensitivity to the strain rate. The material properties for long rods and targets are listed in Appendix A. This material model was successful in predictions of the final parameters of the penetration process [20-22].

Investigations according to simulations yielded some important outcomes, which constituted the basis for using the W-A model and making appropriate changes into the model for the analysis of eroding penetration of long rods into concrete targets. These results are as follows:

a. When the initial velocity is large enough to satisfy Taylor's test conditions (Normal impacting of deformable rod against a rigid target [23]), an increase in striking velocity causes the plastic region to grow. This reaction appears at velocities lower than 500m/s for the copper projectiles examined in this research. Deformations in the target and the projectile under such

conditions are shown in Figure 3 in which a copper rod with a length of 5 cm and diameter of 0.4 cm strikes a concrete target at 348 m/s (experiment performed by these authors).

b. Shock wave circumstance at the tip of the projectile results in a reflection of the stress wave after reaching the boundary of the plastic region and prevention of growth of the plastic region in the projectile when velocity of the impact is increased from 500 m/s to 2500 m/s. In other words, the plastic region cannot grow any further; hence the decrease in linear momentum is mainly due to a reduction in projectile mass rather than resistant forces. A schematic view of the shock situation at earlier stages of penetration is shown in Figure 4. Results of the impact of a copper projectile with a length 5 cm and a diameter of 0.4 cm impacted the concrete target at 648 m/s as shown in Figure 5. Evidence of an intact portion of the projectile in the figure indicates that erosion occurred before plastic flow.

c. Increased velocity of the impact results in growth of the plastic region in the concrete target, which in turn enlarges its incompressible region. Relevant increases in velocity of the impact and thickness of the plastic region obtained from simulations are shown in Figure 6.

d. Regarding high velocity impacts greater than 1000 m/s, all simulations show only a small change in velocity of penetration and velocity of the non-deforming part of the projectile (with respect to initial velocity during most of the process). A severe drop in velocity, which results in projectile stop, occurs at the end of penetration due to mass consumption.

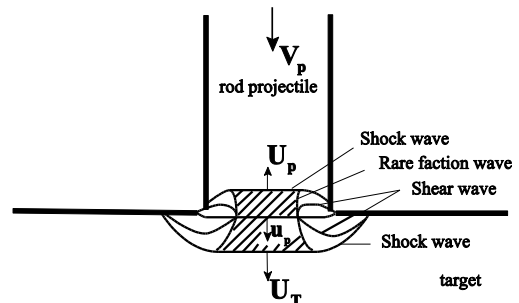


Figure 4. Erosion initiation in projectile due to prevention of plastic flow growth by shock front [19]

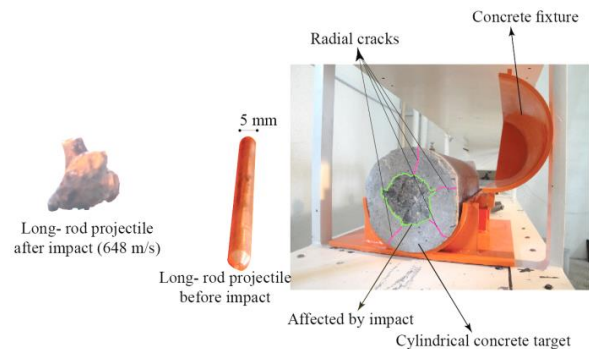


Figure 5. Results of copper projectile impact on concrete target at 648m/s

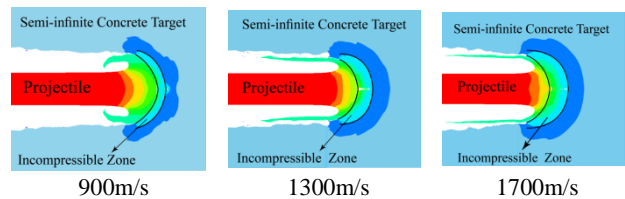


Figure 6. Configuration of the incompressible region ahead of eroding projectile tip during penetration into the concrete target at different impact velocities (simulation).

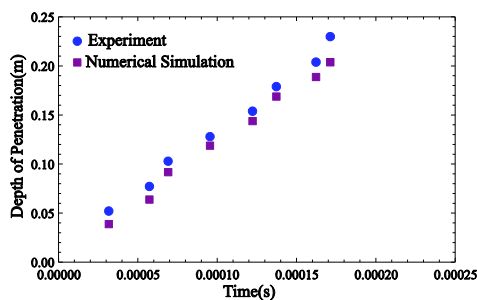


Figure 2. Time history of penetration depth from simulation and experiment [16]

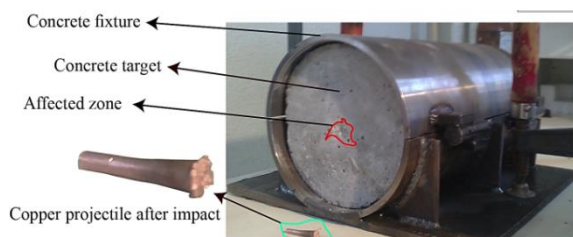


Figure 3. Growth of the plastic region in copper projectile during after striking a concrete target at 348m/s

This reaction to velocity became more visible with increase in velocity of the impact.

e. Material flow from the copper projectile tip occurs completely and approaches a steady state for velocities greater than 1000 m/s. This phenomenon is clearly visible in Figure 6. At velocities between 1500 m/s and 1700 m/s the effects of rigidity and erosion interact so that the maximum depth of penetration is achieved. In other words, an optimum velocity may exist there at which the penetration depth is maximized whereby in the lower velocity region the penetration is dominated by the penetrator rigid body motion. For the copper projectile used in the simulation, rigidity is dominant compared with levels of pressure applied by the tip of the projectile to the target. Therefore, an increase in the velocity of the impact results in an increased depth of penetration; while at greater velocities, the range of velocity increases causing more

erosion and consequently, steady-state penetration occurs independently of the velocity of the projectile.

**4. FORMULATION OF ERODING PENETRATION OF A LONG-ROD PROJECTILE AT A SEMI-INFINITE CONCRETE TARGET**

Results of investigations by simulations showed that responses to concrete penetration (for parameters such as erosion, decrease in rod velocity, cavity generation mechanism at the steady part of penetration and pressure circumstance at the projectile-target interface) were generally similar to responses to penetration in metallic targets<sup>12</sup>[16, 22, 24, 25]. In other words, velocity fields at the projectile tip for eroding penetration into metallic and concrete targets have meaningful similarities. Hence, in order to obtain a plastic flow field, it is possible to use the same potential responses of metals for concrete targets. It is important to note that these similarities were not evident on a microscopic scale or at pressures less severe. Therefore, the arguments presented in this paper are only valid for those cases in which eroding penetration-induced pressure results in total elimination of porosity in concrete and when the reaction of concrete is like that of a nonporous material and its flow behavior is that of metal flow [22, 25]. This condition is considered in equations of state in these simulations so that its different parts are related to different porous and non-porous parts of the target<sup>1</sup>.

For the analysis of penetration of an eroding long rod into a concrete target the necessary changes are inserted in W-A equations<sup>1</sup> and then the resulting equations are solved which are generally in the same form as the original equations but with a different nature for some parameters. The momentum Equation (1) at axial direction Z in Cartesian coordinate system is as follows<sup>1</sup>:

$$\rho \left( \frac{\partial v_z}{\partial t} + v_x \frac{\partial v_z}{\partial x} + v_y \frac{\partial v_z}{\partial y} + v_z \frac{\partial v_z}{\partial z} \right) = \frac{\partial \sigma_{xz}}{\partial x} + \frac{\partial \sigma_{yz}}{\partial y} + \frac{\partial \sigma_{zz}}{\partial z} \quad (8)$$

Considering axial symmetry, specifying velocity changes at axial direction (from the simulation), determining flow and plastic behavior, determining deceleration of the rigid part of the projectile and substituting in Equation (8) and then, integrating along the projectile axis from the end tail of the projectile to semi-infinite result in the following equations for strength, deceleration and rod erosion, respectively [Detailed in Appendix A]:

$$\rho_p \dot{v}(\ell-s) + \dot{u} \left\{ \rho_p s + \rho_t R \frac{\alpha-1}{\alpha+1} \right\} + \rho_p \left( \frac{v-u}{s} \right) \frac{s^2}{2} + \rho_t \dot{\alpha} \frac{2Ru}{(\alpha+1)^2} = \frac{1}{2} \rho_p (v-u)^2 - \left\{ \frac{1}{2} \rho_t u^2 + \frac{7}{3} \ln(\alpha) y_t \right\} \quad (9)$$

$$\dot{v} = -\frac{y_p}{\rho_p(\ell-s)} \left\{ 1 + \frac{v-u}{c_w} + \frac{\dot{s}}{c_w} \right\} \quad (10)$$

$$\dot{\ell} = -(v-u) \quad (11)$$

**5. MODIFICATION OF THE W-A MODEL: CALCULATION OF  $\alpha$  (THICKNESS OF THE INCOMPRESSIBLE REGION AHEAD OF THE PROJECTILE TIP BASED ON VISCOPLASTIC BEHAVIOR) AND IN EQUATION (9) FOR CONCRETE TARGETS**

The most complicated part of penetration mechanics is the accurate determination of fields of stress and velocity in a target and the effects of these two parameters which have important roles in describing the level of a target's resistance. These are reflected in parameter  $\alpha$  (representing strength, viscosity and plastic flow of concrete under high pressure, strain rates and confinement as in Figure 7). Therefore, correct and accurate calculation of parameter  $\alpha$  enables the W-A equations to be solved explicitly via the analysis of penetration into a concrete target. A detailed explanation of characteristics and the method of attributing plastic flow field properties to this parameter are associated with the mechanism of resistance against penetration, represented in reference [16]. Thickness of the incompressible region and the concept of parameter  $\alpha$  are shown in Figure 7.

The value of thickness  $\Delta$  or subsequent  $\alpha$  are calculated according to viscoplastic behavior. For viscoplastic materials, stress is defined as:

$$\sigma = \begin{cases} -p(\rho)\mathbf{I} + \left( 2\eta(\rho) + \frac{k(\rho)}{\sqrt{II_D}} \right) \mathbf{D} & \text{for } \mathbf{D}' \neq 0, \\ -p(\rho)\mathbf{I} & \text{for } \mathbf{D}' = 0 \end{cases} \quad (12)$$

The first part of Equation (12) describes flow stress and the last part defines the behavior of concrete when the particles are subjected to pressure without any flow. In order to determine the movement of particles in the compressible region, equations of mass and conservation of momentum associated with the viscoplastic constitutive equation are solved simultaneously. These equations are as follows:

$$\begin{cases} \text{div } \sigma = \rho \mathbf{a} \\ \text{div } \mathbf{v} = 0 \\ \sigma = \sigma \mathbf{I} + \left( 2\eta + \frac{k}{\sqrt{II_D}} \right) \mathbf{D} \end{cases} \quad (13)$$

Converting the parameters into dimensionless form and inserting boundary conditions at the cavity surface and at the end of the compressible region, obtain the radial, circumferential and shear components of stress in the incompressible region [26]:

1. Autodyn 6.1 Material Library 2006

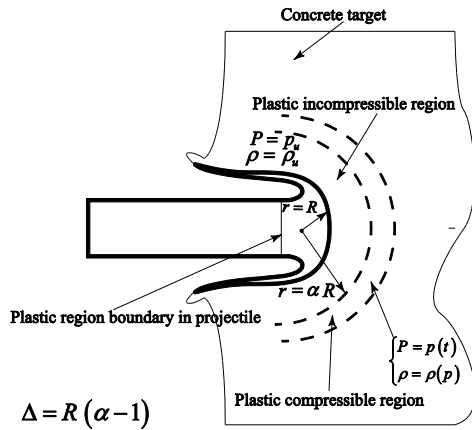


**Figure 7.** Conformation of compressible and incompressible plastic regions in concrete target subjected to eroding penetration of long rod

$$\bar{\sigma}_n(x(\tau), \tau) = 2\bar{k}\sqrt{3}\text{sgn}f(\tau)\left(\ln x - \frac{1}{3}\right) - 4\bar{\eta}\frac{f'(\tau)}{x^3} + M_u^2\left[\frac{V_*f'(\tau)}{V_0x} + \frac{1}{2}\frac{f(\tau)^2}{x^4}\right] + F(\tau) \quad (14a)$$

$$\bar{\sigma}_{\theta\theta}(x(\tau), \tau) = \bar{\sigma}_{\phi\phi}(x(\tau), \tau) = \bar{k}\sqrt{3}\text{sgn}f(\tau)\left(\ln x + \frac{1}{3}\right) + 2\bar{\eta}\frac{f'(\tau)}{x^3} + M_u^2\left[\frac{V_*f'(\tau)}{V_0x} + \frac{1}{2}\frac{f(\tau)^2}{x^4}\right] + F(\tau) \quad (14b)$$

$$\bar{\sigma}_{r\theta}(x(\tau), \tau) = 2\bar{k}\sqrt{3}\text{sgn}f(\tau)\ln x + M_u^2\left[\frac{V_*f'(\tau)}{V_0x} + \frac{1}{2}\frac{f(\tau)^2}{x^4}\right] + F(\tau) \quad (14c)$$

Functions  $f(\tau)$  and  $F(\tau)$  are time-dependent functions that arise during integration and are determined from shock wave conditions and stresses at the boundaries of the incompressible region, respectively. Function  $f'(\tau)$  is the time derivative of  $f(\tau)$ . Furthermore, parameters  $M_u$  and  $V_*$  are defined as  $M_u = \rho_u V_0^2 / \rho_0$  and  $V_* = R/t_{ad}$ , respectively. Thickness of the plastic region, which constitutes the thickness of the layer and whose particle pressure is beyond the lock pressure of concrete, is obtained as follows:

$$2\bar{k}\sqrt{3}\text{sgn}f(\tau)\ln x_m - 4\bar{\eta}f(\tau)\left[\frac{1}{x_m^3} - 1\right] + M_u^2\left[\frac{V_*}{V_0}\right]f'(\tau)\left[\frac{1}{x_m} - 1\right] + M_u^2\frac{1}{2}f^2(\tau)\left[\frac{1}{x_m^4} - 1\right] = \bar{P}(\tau) - \bar{p}_u \quad (15)$$

The roots of Equation (15) give the thickness of the incompressible layer at different times. In other words, parameter  $X_m = X(\tau)$  is time dependent. As explained in reference [16], the maximum value of  $X_m$  is obtained at  $\tau=1$ . It is clear from Figure 7 that  $X_m(1) = \alpha$ . The parameter  $\alpha$  describes the thickness of the incompressible layer based on compressibility and viscosity properties of concrete. After calculation of the value  $\alpha$ , which is the most important parameter for determining penetration behavior in the W-A model, equations are solved in order to establish penetration of

an eroding long-rod into the semi-infinite concrete target.

The value of  $y_i$  in the Equation (9) is very important. Based on experiments (performed by authors in reference [24]) and comparing their results with the presented model and using the approach presented in reference [15],  $y_i$  was considered as  $y_i = (R/r)^2 f'_c$ . Results of this approach are in good agreement with those presented in reference [15] and show an increase in target strength due to eroding penetration up to four to five times its initial value.

## 6. SOLUTION OF EQUATIONS OF PENETRATION OF A HIGH-VELOCITY ERODING LONG ROD INTO CONCRETE TARGETS

Simultaneous solution of Equations (9)-(11) and (15) results in a time history of penetration depth, projectile velocity and penetration velocity of the eroding projectile into the concrete target. The complete solution depends on knowing initial penetration velocity, which is obtained from shock wave conditions at the beginning of penetration, shown schematically in Figure 4. The relation of shock wave propagation velocity to velocity of the concrete particle is determined as [27]:

$$U = C + Su \xrightarrow{\text{for typical concrete}} U_i = 2.76u + 1945 \quad (16)$$

Shock conditions are rewritten considering the interaction between projectile and target [4]:

$$U_t = C_t + S_t u_t \quad (17)$$

$$v_0 - U_p = C_p + S_p (v_0 - u_0) \quad (18)$$

Subscripts  $t$  and  $p$  denote target and projectile, respectively. Using jump conditions at the shock wave front, the following can be written:

$$p_t = \rho_t U_t u_0 \quad (19)$$

$$p_p = \rho_p (v_0 - U_p)(v_0 - u_0) \quad (20)$$

Equating the last two equations and substituting Equations (17) and (18) result in:

$$u_0 = \frac{b - \sqrt{b^2 - 4ac}}{2a} \quad (21)$$

where:

$$a = S_p - S_t \frac{\rho_t}{\rho_p}, \quad b = 2S_p v_0 + C_p + C_t \frac{\rho_t}{\rho_p}, \quad c = C_p v_0 + S_p v_0^2 \quad (22)$$

When material properties are known<sup>23</sup>, the penetration problem is ready to be solved. In order to solve time-dependent equations, a program was written so that

Equations (9-11) were expressed as explicit functions of time:

$$v = v + f(\underbrace{\alpha, c_w, C_t, C_p, f'_c, \gamma_p, \gamma_t, \rho_p, \rho_t}_{\text{deceleration} \rightarrow f < 0}) dt \tag{23}$$

$$u = u + f(\underbrace{\alpha, c_w, C_t, C_p, f'_c, \gamma_p, \gamma_t, \rho_p, \rho_t}_{\text{deceleration} \rightarrow f < 0}) dt \tag{24}$$

$$l = l - (v - u) dt \tag{25}$$

The properties of flow, viscosity, compressibility and strain rate are included in parameter  $\alpha$ . It is necessary to mention that the valid time interval for a solution of Equation (15) is the one prior to reaching a steady condition in the thickness of the incompressible layer.

### 7. HIGH VELOCITY IMPACT TESTS

52 high-velocity impact tests were performed using a one-stage gas gun in order to study penetration of the eroding long-rod penetrators into the concrete targets. Some tests failed due to buckling. Details of tests are in reference [24]. Among the 52 tests 12 of them were opted in order to validate the presented model. Some projectiles before and after impact are shown in Figure 8.

The values for the parameter of unconfined compression strength in these tests were 51.9MPa and 39MPa, respectively. The comparison between the results of the presented model and the result of the tests are shown in the Figures 9 & 10. In both cases, the experimental results are placed at the top of the analytical curves, because the target material had suddenly lost its resistance against the penetration (in fact compressive stress waves reflected from the free surface of the cylinder in tension was what gave rise to the collapse of the target) [24].

The values for the parameter of unconfined compression strength in these tests were 51.9MPa and 39MPa, respectively. The comparison between the results of the presented model and the result of the tests are shown in the Figures 9 & 10. In both cases, the experimental results are placed at the top of the analytical curves, because the target material had suddenly lost its resistance against the penetration (in fact compressive stress waves reflected from the free surface of the cylinder in tension was what gave rise to the collapse of the target) [24].

It is noted that considering the large-scale heterogeneity of concrete material, it is problematic to recommend an exact analytical model but it seems that the presented model can be a suitable approximation for parametric studies.

In order to evaluate the presented model, the time variations according to projectile length, penetration depth, projectile velocity and penetration velocity for impact of a copper long rod with a length of 19 cm and length to diameter ratio of 14.7 against a semi-infinite cylindrical concrete are shown in Figures (11-14). The rationale for adopting such a model is reflected in the valuable experiment result [14]. In addition, it allows the evaluation of the presented model in ranges of velocity and mass that were not possible in the experiments of the authors.

It is apparent that validating the time history for the time taken for penetration is adequate for reliability of instantaneous length of projectile, penetration velocity and projectile rod velocity. As can be seen in Figures (11-14), there is a steady-state condition during most of the penetration time and the process becomes unsteady only at the first and final steps of penetration.



Figure 8. Residual projectiles after impact

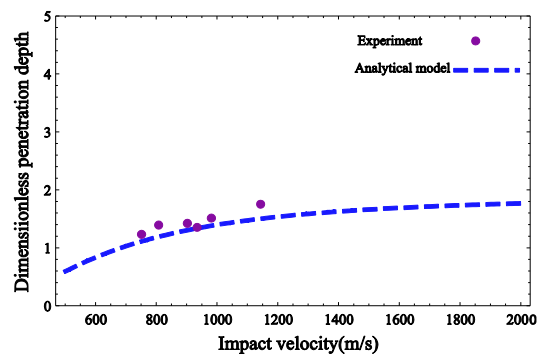


Figure 9. Impact velocity- dimensionless penetration depth ( $f'_c=51.9$  MPa and  $L=50$ mm& $d=5$ mm)

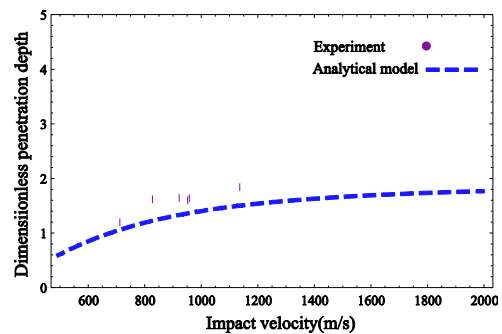


Figure 10. Impact velocity- dimensionless penetration depth ( $f'_c=39$  MPa and  $L=50$ mm& $d=5$ mm)

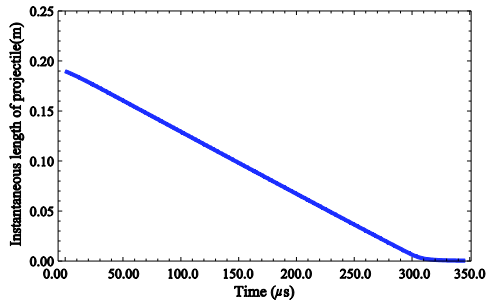


Figure 11. Time history of projectile length during penetration into concrete

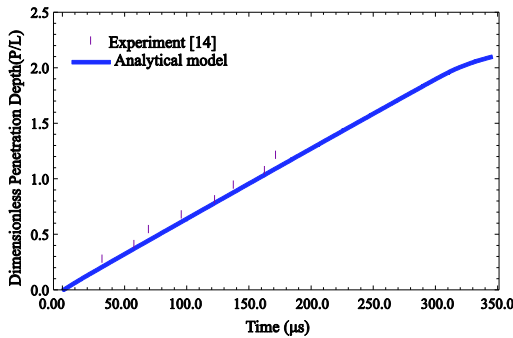


Figure 12. Time history of depth of penetration into concrete

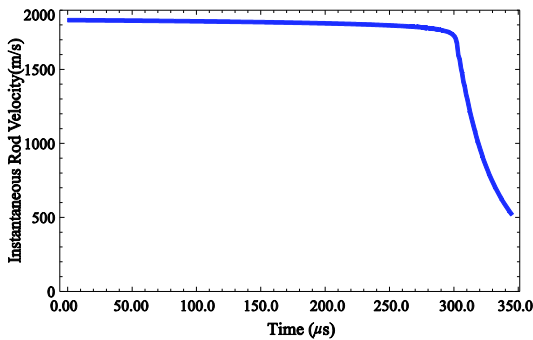


Figure 13. Variations of velocity of non-deformed part of the projectile during penetration into concrete

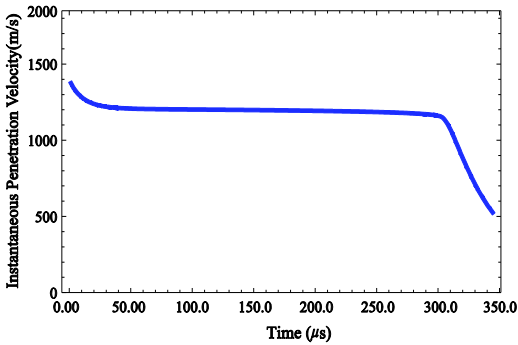


Figure 14. Variations of penetration velocity during penetration into concrete

### 8. PARAMETRIC STUDY

It was shown in the previous sections that the proposed model can analyze penetration of an eroding long rod into a concrete target. Now, a parametric study is performed in order to evaluate the more effective parameters from those results. Sensitivity analysis of effective parameters of the model showed that the two parameters, compressive strength and  $\alpha$ , have the largest effects on model predictions. This result was expected because the parameter of compressive strength is the most dominant component affecting the strength of concrete and  $\alpha$  is representative of concrete flow under high pressure and high strain rate conditions. Effects of these two parameters on the results of the model are shown in Figures 15 and 16. Figure 15 shows that when the value of  $\alpha$  exceeds a specific limit, considerable changes take place in the depth of penetration and therefore in resistance against the penetration.

This means that the critical limit for  $\alpha$  must be considered in designs for concrete structures. Figure 16 shows that there is a maximum depth of penetration when  $f'_c$  has a specific value. This is similar to the behavior of Tate's curves when the target strength is greater than the projectile strength except that quantities

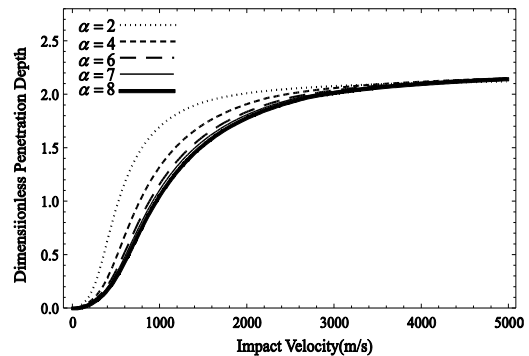


Figure 15. Effect of the parameter  $\alpha$  on variations of penetration depth versus striking velocity

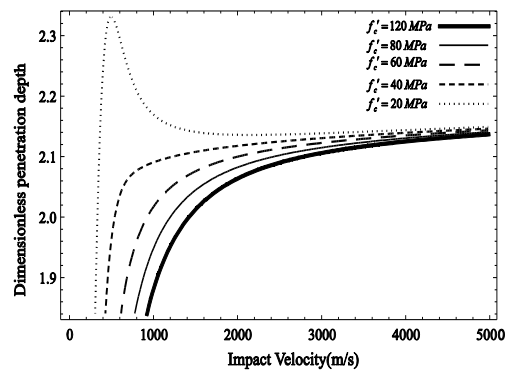


Figure 16. Effect of the parameter  $f'_c$  on penetration depth-striking velocity curve

are completely different for concrete because specific responses of concrete are reflected by means of parameter  $\alpha$ . In addition, the comparison between Figures 15 and 16 clearly shows the scale of the effect of  $\alpha$  on the concrete's resistance compared with  $f_c'$ . This comparison shows that the effect of  $\alpha$  on the strength of concrete is not less than  $f_c'$ . In other words, in order to increase the resistance of concrete to penetration of high-velocity projectiles, improving both  $\alpha$  and  $f_c'$  is better than increasing only  $f_c'$ .

## 9. CONCLUDING REMARKS

In recent years, numerical methods and concrete material models have improved, hence it is possible to simulate the penetration of an eroding projectile into a concrete target in precise details but it must be noted that the use of an analytical model is unavoidable, because parametric studies and some important design considerations are very difficult and time-consuming by numerical simulations. However, the W-A model proposed about 20 years ago has a rigorous basis (flow field) and can be realized as a reference model after the Tate model in erosive penetration.

The improved W-A model for analysis of penetration of high-velocity eroding projectiles into concrete targets has been presented in this paper. The model was based on the improvement of the method of calculating the plastic flow field of concrete in terms of its specific functions such as compressibility and viscosity under conditions of high pressure. The flow field is calculated using the viscoplastic constitutive equation and is thus substituted into the W-A model. Solving these equations results in an analytical approach which is appropriate for the analysis of stages of eroding penetration into concrete targets. In general, it can be stated that:

- High-velocity penetrations into metallic and concrete targets are generally similar. The good agreement between the results of analysis and the experimental results supports this idea.
- The best approach to derive an erosive penetration into concrete target equation is the flow field approach (i.e., analysis of the flow field around the projectile tip during the penetration process).
- Consideration of the erosion equation in high-velocity penetration into concrete targets is inevitable. Hence, the Forrestal family of models (that assume a projectile is rigid) are not able, even as an approximation, to calculate principal penetration parameters in an eroding penetration
- Considering the large-scale heterogeneity of concrete targets (i.e., the random aggregates and the particles embedded), it is problematic to recommend an exact analytical model for analyzing penetration of an

eroding projectile into such targets. Therefore, some discrepancies between an analytical model and test results are acceptable and must not be compared with penetration into a metallic target (Figures 9 & 10).

- The role of  $f_c'$  becomes less important when the impact velocity increases and penetration resistance is determined by a combination of several parameters such as impact velocity, viscosity and flow at high strain rates which are included in parameter  $\alpha$ .
- Penetration velocity and projectile rod velocity have very small variations (which can be easily improved) during most of the penetration process. A sudden drop in velocity at the final stage of penetration occurred due to an overall decrease in mass rather than pressure from resistance. Projectile rod erosion is a completely local and plastic region in the projectile concentrated in a small region of its tip, and elastic waves do not move along a projectile axis due to shock conditions. Therefore, penetration equations have approximately steady conditions.
- A correct description of the plastic flow field in a concrete target (by numerical simulations using improved material models such as RHT to investigate precise details of flow field specifications) resulted in a real analysis of the reaction of concrete to penetration. Therefore, representing more precise penetration models involves the correct and precise description of constitutive equations and plastic flow fields of concrete.

## 10. ACKNOWLEDGEMENTS

The authors gratefully acknowledge the funding by Arak University, under grant No 92/12106

## 11. REFERENCES

1. Tate, A., "Long rod penetration models—part i. A flow field model for high speed long rod penetration", *International Journal of Mechanical Sciences*, Vol. 28, No. 8, (1986), 535-548.
2. Vahedi K., "Developments of an analytical method for ballistic impact of long-rod penetrators", Doctoral dissertation, (1991), Louisiana Technology University.
3. Luk, V. and Piekutowski, A., "An analytical model on penetration of eroding long rods into metallic targets", *International Journal of Impact Engineering*, Vol. 11, No. 3, (1991), 323-340.
4. Roisman, I., Yarin, A. and Rubin, M., "Normal penetration of an eroding projectile into an elastic-plastic target", *International Journal of Impact Engineering*, Vol. 25, No. 6, (2001), 573-597.
5. Rubin, M. and Yarin, A., "A generalized formula for the penetration depth of a deformable projectile", *International Journal of Impact Engineering*, Vol. 27, No. 4, (2002), 387-398.
6. Forrestal, M., Altman, B., Cargile, J. and Hanchak, S., "An empirical equation for penetration depth of ogive-nose

- projectiles into concrete targets", *International Journal of Impact Engineering*, Vol. 15, No. 4, (1994), 395-405.
7. Forrestal, M. and Tzou, D., "A spherical cavity-expansion penetration model for concrete targets", *International Journal of Solids and Structures*, Vol. 34, No. 31-32, (1997), 4127-4146.
  8. Forrestal, M., Frew, D., Hickerson, J. and Rohwer, T., "Penetration of concrete targets with deceleration-time measurements", *International Journal of Impact Engineering*, Vol. 28, No. 5, (2003), 479-497.
  9. Gao, S., Jin, L. and Liu, H., "Dynamic response of a projectile perforating multi-plate concrete targets", *International Journal of Solids and Structures*, Vol. 41, No. 18, (2004), 4927-4938.
  10. Gao, S.-q., Liu, H.-p., Li, K.-j., Huang, F.-l. and Jin, L., "Normal expansion theory for penetration of projectile against concrete target", *Applied Mathematics and Mechanics*, Vol. 27, No. 4, (2006), 485-492.
  11. Shiqiao, G., Lei, J., Haipeng, L., Xinjian, L. and Li, H., "A normal cavity-expansion (NCE) model based on the normal curve surface (NCS) coordinate system", *International Journal of Applied Mathematics*, Vol. 37, No. 2, (2007).
  12. Shiqiao, G., Haipeng, L. and Lei, J., "A fuzzy model of the penetration resistance of concrete targets", *International Journal of Impact Engineering*, Vol. 36, No. 4, (2009), 644-649.
  13. Gold, V. M., "Analysis of the penetration resistance of concrete", (1997), DTIC Document.
  14. Gold, V. M., Vradis, G. C. and Pearson, J. C., "Concrete penetration by eroding projectiles: Experiments and analysis", *Journal of Engineering Mechanics*, Vol. 122, No. 2, (1996), 145-152.
  15. Rosenberg, Z. and Dekel, E., "A numerical study of the cavity expansion process and its application to long-rod penetration mechanics", *International Journal of Impact Engineering*, Vol. 35, No. 3, (2008), 147-154.
  16. Nia, A. A., Zolfaghari, M., Mahmoudi, A., Nili, M. and Khodarahmi, H., "Analysis of resistance of concrete target against penetration of eroding long rod projectile regarding flow field around the projectile tip", *International Journal of Impact Engineering*, Vol. 57, (2013), 36-42.
  17. Anderson, C. E. and Walker, J. D., "An examination of long-rod penetration", *International Journal of Impact Engineering*, Vol. 11, No. 4, (1991), 481-501.
  18. Anderson, C. and Walker, J., "Long-rod penetration and the calculation of target resistance", *Shock Compression of Condensed Matter Elsevier publishers*, (1991), 967-970.
  19. Cleja-Tigoiu, S., Cazacu, O. and Tigoiu, V., "Dynamic expansion of a spherical cavity within a rate-dependent compressible porous material", *International Journal of Plasticity*, Vol. 24, No. 5, (2008), 775-803.
  20. Gebbeken, N. and Ruppert, M., "A new material model for concrete in high-dynamic hydrocode simulations", *Archive of Applied Mechanics*, Vol. 70, No. 7, (2000), 463-478.
  21. Tu, Z. and Lu, Y., "Modifications of rht material model for improved numerical simulation of dynamic response of concrete", *International Journal of Impact Engineering*, Vol. 37, No. 10, (2010), 1072-1082.
  22. Tu, Z. and Lu, Y., "Evaluation of typical concrete material models used in hydrocodes for high dynamic response simulations", *International Journal of Impact Engineering*, Vol. 36, No. 1, (2009), 132-146.
  23. Zukas, J. A., "High velocity impact dynamics, Wiley-Interscience, (1990).
  24. Nia, A. A., Zolfaghari, M., Khodarahmi, H., Nili, M. and Gorbakhani, A. H., "High velocity penetration of concrete targets with eroding long-rod projectiles; an experiment and analysis", *International Journal of Protective Structures*, Vol. 5, No. 1, (2014), 47-63.
  25. Dowling, N. E., "Mechanical behavior of materials, Pearson, (2012).
  26. Walker, J. D. and Anderson, C. E., "A time-dependent model for long-rod penetration", *International Journal of Impact Engineering*, Vol. 16, No. 1, (1995), 19-48.
  27. Gebbeken, N., Greulich, S. and Pietzsch, A., "Hugoniot properties for concrete determined by full-scale detonation experiments and flyer-plate-impact tests", *International Journal of Impact Engineering*, Vol. 32, No. 12, (2006), 2017-2031.

## Modifications to Walker-Anderson Model for Analysis of High-velocity Penetration of an Eroding Long-rod Projectile into Semi-infinite Concrete Targets

M. Zolfaghari

Department of Mechanical Engineering, Arak University, Arak, Iran

### PAPER INFO

چکیده

#### Paper history:

Received 12 July 2016

Received in revised form 08 August 2016

Accepted 10 March 2017

#### Keywords:

Eroding Projectile  
Concrete Resistance  
Analytical Model  
Long Rod  
Penetration

در این مقاله مدل تغییر شکل یافته والکر- اندرسون جهت تحلیل نفوذ یک پرتابه فرسایشی در یک هدف بتنی ارائه می‌شود. بهبود صورت گرفته در مدل W-A مربوط به محاسبات جریان پلاستیک بتن با در نظر گرفتن تراکم پذیری و حساسیت به نرخ کرنش است. بر این اساس معادلات نفوذ با تغییرات مربوط به میدان پلاستیک بازنویسی شده است و حل معادلات پارامترهای عمق نفوذ، سرعت میله پرتابه، طول پرتابه، را به صورت لحظه‌ای در اختیار قرار می‌دهد. نتایج این تحلیل با آزمایش‌های صورت گرفته توسط مولفان این مقاله مقایسه شده است. آزمایش‌ها برای میله پرتابه‌هایی با نسبت طول به قطر  $9 \leq L/d \leq 11$  در اهداف نیمه بی‌نهایت بتنی برای سرعت‌های برخورد بالا ( $650 \leq V \leq 1150$ ) صورت گرفته است. مقایسه نتایج مدل تحلیلی و آزمایشات تطابق کلی نتایج آزمایش‌ها و مدل را نشان می‌دهد (میانگین خطا ۱۲٪). در مواردی که امکان آزمایش تجربی وجود نداشت، مدل بهبود یافته با نتایج شبیه‌سازی‌های صورت گرفته توسط نویسندگان مقایسه گردید. مطالعات پارامتریک صورت گرفته نشان داد دو پارامتر مشخصه جریان پلاستیک در نوک پرتابه  $\alpha$  و استحکام نامحدود فشاری بتن دو پارامتر کلیدی تاثیر گذار بر نتایج هستند. این مطالعه نشان داد مرتبه اهمیت مشخصه میدان جریان پلاستیک در شکل گیری مقاومت در برابر نفوذ کمتر از تاثیر مقاومت نامحدود فشاری بتن نیست.

doi: 10.5829/idosi.ije.2017.30.05b.18